

An Investigation into the Cytotoxicity and Mode of Action of Some Novel *N*-Alkyl-Substituted Isatins

Kara L. Vine,^{*,†,‡} Julie M. Locke,[‡] Marie Ranson,[†] Stephen G. Pyne,[‡] and John B. Bremner[‡]

School of Biological Sciences, and Department of Chemistry, University of Wollongong, NSW 2522, Australia

Received April 10, 2007

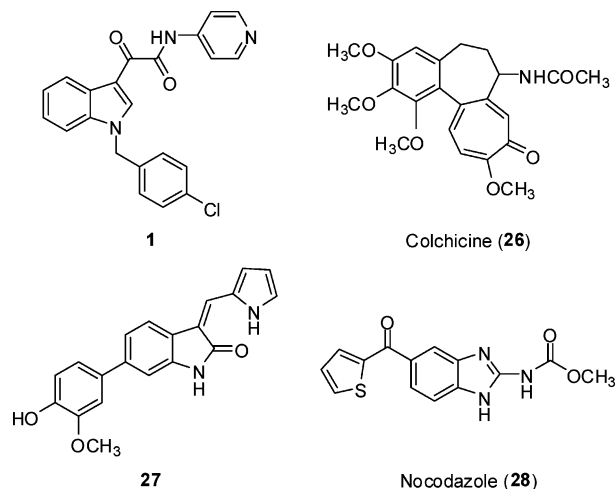
A range of substituted *N*-alkylisatins were synthesized and their cytotoxicity evaluated against several cancer cell lines *in vitro*. SAR studies indicated that the introduction of an aromatic ring with a one or three carbon atom linker at N1 enhanced the activity from that of the allyl, 2'-methoxyethyl, and 3'-methylbutyl *N*-substituted isatins. Furthermore, electron-withdrawing groups substituted at the meta or para position of the ring were favored over the ortho orientation. Of the 24 compounds screened, nine displayed sub-micromolar IC₅₀ values and in general demonstrated greater selectivity toward leukemia and lymphoma cell lines over any of the carcinoma cell lines tested. 5,7-Dibromo-*N*-(*p*-methylbenzyl)isatin (**6**) was the most active compound, inhibiting the metabolic activity of both U937 and Jurkat cancer cell lines at 0.49 μM. Various *N*-alkylisatins were also found to dramatically alter lymphocyte morphology, destabilize microtubules, inhibit tubulin polymerization, induce G2/M cell cycle arrest, and activate the effector caspase-3 and -7.

Introduction

The isatin molecule (1*H*-indole-2,3-dione) is a versatile moiety that displays diverse biological activities,¹ including anticancer activity.^{2,3} The synthetic flexibility of isatin has led to the synthesis of a variety of substituted derivatives; however, the susceptibility of isatin to attack by nucleophiles at C3 has resulted in the generation of a large number of 3-substituted isatins in particular. This is reflected by numerous biologically active 3-substituted indolin-2-ones that are reported in the literature.^{4–6} Despite the significant amount of anticancer research being devoted to this chemical class, it should not be assumed that 3-substituted isatins are richer in bioactivity than other 1*H*-indole-2,3-dione derivatives. *N*-Alkylated indoles have also been reported to exhibit anticancer activity. For example, the indolyl amide D-24851 (**1**) has been found to block cell cycle progression in a variety of malignant cell lines including those derived from the prostate, brain, breast, pancreas, and colon.⁷ *In vivo*, compound **1** proved efficacious in a rat Yoshida AH13 sarcoma model and induced complete tumor regression and curative treatment of the animals, with no toxic side effects.⁷ Structurally related compounds have also been reported to activate caspases in a cytochrome *c*-dependent manner and therefore induce apoptosis in cancer cell lines but not normal cells.⁸ Furthermore, Liu and colleagues identified a class of isatin *O*-acyl oximes that selectively inhibited neuronal ubiquitin C-terminal hydrolase (UCH-L1) in a H1299 lung cancer cell line, which is proposed to be linked to tumor progression upon upregulation.⁹

Although very few studies have described SARs^a attributable to modifications to the benzene ring of isatin,^{2,9,10} we have previously shown that the introduction of electron-withdrawing groups to the benzene ring is associated with increased biological activity for a range of indole-based compounds.³ Given this,

the aim of the current study was to screen a range of *N*-alkylated isatins including those with both aliphatic and aromatic substituted groups, as well as different bromine substitution patterns on the isatin moiety, for cytotoxicity against a panel of cancer cell lines and to determine the SAR. A further aim was to investigate the biological mode of action using a range of cell-based and cell-independent approaches. The results of this work are reported herein.



Results and Discussion

Chemistry. The structures of the *N*-alkylated isatins synthesized are shown in Table 1. Several methods have been employed to produce *N*-alkylated isatins. Generally, the isatin is exposed to an alkylating agent in the presence of a base. For our purposes, the alkylation of the isatins was carried out using the general method shown in Scheme 1, with Cs₂CO₃ or K₂CO₃ employed as a base. This procedure was based on a method by Torres,¹¹ which was reported to give good yields with 7-substituted isatins. Formation of the dark violet isatin anion was more facile when Cs₂CO₃ was used; however, the yields of final product were comparable using either base. The time required for the alkylation reaction varied depending upon

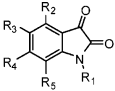
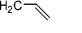

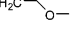
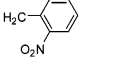
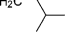

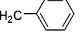



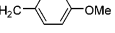

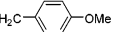

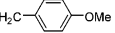
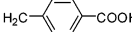
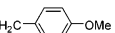
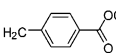
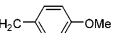
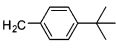
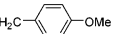
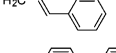
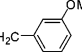
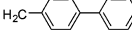
* To whom correspondence should be addressed. Telephone: +61 (0)2 42214356. Fax: +61 (0)2 42214135. E-mail: klv04@uow.edu.au.

[†] School of Biological Sciences.

[‡] Department of Chemistry.

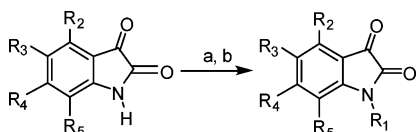
^a Abbreviations: SAR, structure activity relationship; PBL, peripheral blood lymphocyte; MDR, multi-drug resistance; EDTA, ethylenediamine-tetraacetic acid.

Table 1. Cytotoxicity of Isatin Derivatives **2–25** on U937,^a Jurkat,^b and MCF-7^c Cells As Calculated from Dose Response Curves^d

Compound	R ₁	R ₂	R ₃	R ₄	R ₅	IC ₅₀ (μM) ^e			Compound	R ₁	R ₂	R ₃	R ₄	R ₅	IC ₅₀ (μM) ^e		
						U937	Jurkat	MCF-7							U937	Jurkat	MCF-7
																	
2		H	Br	H	Br	6.67	NT ^f	NT	14		H	Br	H	Br	0.89	0.89	4.32
3		H	Br	H	Br	3.44	8.95	6.67	15		H	Br	H	Br	2.27	NT	3.18
4		H	Br	H	Br	2.40	3.47	7.49	16		H	Br	H	Br	0.98	0.50	3.87
5		H	Br	H	Br	1.14	1.14	7.09	17		H	Br	H	Br	0.63	0.63	5.27
6		H	Br	H	Br	0.49	0.49	11.0	18		H	Br	H	Br	2.30	0.58	4.22
7		H	H	H	H	>46.8	NT	NT	19		H	Br	H	Br	0.80	0.69	7.13
8		Br	H	H	H	>36.1	NT	NT	20		H	H	Br	H	5.21	5.21	NT
9		H	Br	H	H	>36.1	NT	NT	21		H	Br	H	Br	>14.2	>14.2	>14.2
10		H	H	Br	H	34.1	NT	NT	22		H	Br	H	Br	1.19	1.19	9.05
11		H	H	H	Br	17.6	NT	NT	23		H	Br	H	Br	1.13	0.66	2.64
12		H	Br	H	Br	1.83	0.59	5.18	24		H	Br	H	Br	2.37	1.42	7.81
13		H	Br	H	Br	1.76	2.00	2.35	25		H	Br	H	Br	0.76	0.74	4.88
									vinblastine						6.88	NT	NT

^a U937: human monocyte-like, histiocytic lymphoma cell line. ^b Jurkat: human leukemic T-cell line. ^c MCF-7: human mammary gland adenocarcinoma (non-metastatic) cell line. ^d Sigmoidal dose response curves (variable slope) were generated using GraphPad Prism V. 4.02 (GraphPad Software Inc.). ^e Values are the mean of triplicates of at least two independent experiments. ^f NT = not tested.

Scheme 1. General Method for *N*-Alkylation of Isatin Derivatives To Give **2–20** and **22–25**^a



^a (a) K₂CO₃ or Cs₂CO₃ (1.2 equiv), DMF (1 mL per 0.1 mmol of isatin derivative), 1 h, 4 °C, RT; (b) R₁X (1.1 equiv, X = Cl or Br), KI (cat., 0.2 equiv), 80 °C, 5–24 h.

the reactivity of the alkyl halide and so the reaction with allyl bromide to produce **2** required only 4 h for completion, whereas the reaction with the less reactive 1-bromo-3-methylbutane to yield **4** required a much longer reaction time (24 h). The synthesis of the acid **21** was accomplished via hydrolysis of the methyl ester **22** under acidic conditions. The characterization of all compounds was accomplished using ¹H and ¹³C NMR spectroscopy as well as low-resolution EI MS for known compounds and high-resolution EI MS for novel compounds. The purity of all compounds was greater than 95% as determined by RP HPLC (see Supporting Information).

Biological Activity. Cytotoxicity and SAR Analysis. As part of an ongoing effort to identify potent inhibitors of cancer cell proliferation, the prepared *N*-alkylated isatins **2–25** were investigated for cytotoxicity against a range of cancer cell types (Table 1). A structure–activity-based selection process was used to identify several crucial structural requirements needed to enhance cytotoxicity (based on a cell proliferation assay), which were determined initially against three human cancer cell lines

(U937, Jurkat, and MCF-7, Table 1). The general trend observed among the three cell lines indicated that:

(1) Introduction of an aromatic ring with a one carbon atom linker at N1 (e.g., compound **5**) enhanced biological activity by at least a factor of 2 against U937 and Jurkat cell lines as compared to the allyl, 2'-methoxyethyl, and 3'-methylbutyl *N*-substituted isatins (**2–4**), in the 5,7-dibrominated series. However, no significant change in activity was observed for compounds tested against the MCF-7 cell line.

(2) Introduction of electron-withdrawing groups such as the nitro group were favored in the para (**14**) position over the ortho (**15**) orientation, but no significant difference in activity was observed for para (**12**)- or meta (**13**)-substituted methoxy groups.

(3) Introduction of two bromine atoms at C5 and C7 for the *N*-(*p*-methoxybenzyl)isatin series of compounds (**12**) substantially increased biological activity in comparison to the non- (**7**) or mono-brominated (**8–11**) *N*-alkylisatins (Figure 1).

(4) Increasing the carbon chain length from 1 (**5**) to 3 (**24**) resulted in no significant difference in activity against all three cancer cell lines tested.

Focusing on the most active compounds in the 5,7-dibromo-*N*-alkylisatin series, nine were found to exhibit IC₅₀ values in the sub-micromolar range (Table 1). 5,7-Dibromo-*N*-(*p*-methoxybenzyl)isatin (**6**) was the most active compound, inhibiting 50% of the metabolic activity and hence cellular proliferation in both U937 and Jurkat cells at a concentration of 0.49 μM (Table 1). This was 22 times more potent than the unsubstituted 5,7-dibromoisatin,³ thus emphasizing the importance of N1 substitution for cytotoxic activity. In addition, compound **6** was

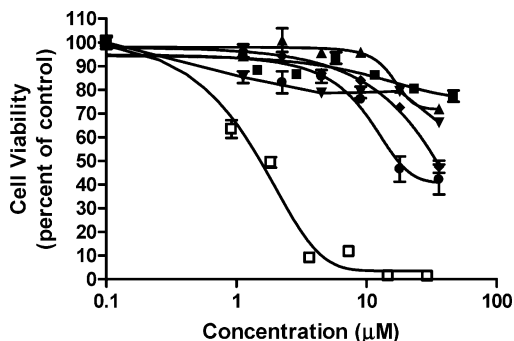


Figure 1. Viability of U937 cells after treatment with different concentrations of (■) *N*-(*p*-methoxybenzyl)isatin (**7**), (▲) 4-bromo-*N*-(*p*-methoxybenzyl)isatin (**8**), (▼) 5-bromo-*N*-(*p*-methoxybenzyl)isatin (**9**), (◆) 6-bromo-*N*-(*p*-methoxybenzyl)isatin (**10**), (●) 7-bromo-*N*-(*p*-methoxybenzyl)isatin (**11**), and (□) 5,7-dibromo-*N*-(*p*-methoxybenzyl)isatin (**12**). Briefly, cells were incubated for 24 h at 37 °C with increasing concentrations of test compound, then analyzed for a change in metabolic activity and expressed as percent viability in reference to the DMSO control. Each data point is a mean of triplicates \pm SE.

>22 times more selective for leukemic (Jurkat) and lymphoma (U937) cancer cell lines than for the breast adenocarcinoma (MCF-7) cell line (Table 1). Five other *N*-alkylisatins (**14**, **16**, **17**, **19**, and **25**) also demonstrated a similar pattern of specificity, but none were as potent as **6**. This effect may be due in part to the expression of the anti-apoptotic Bcl-2 group of proteins that have been identified in MCF-7 cells, for which Bcl-2 and Bcl-X_S expression specifically has been correlated with resistance and poor response to chemotherapy.^{12–15}

Interestingly, activity was compromised in all three cancer cell lines when a carboxylic acid was substituted at the para position of the aromatic ring (**21**, Table 1). Such a decrease in activity was not correlated with electronic (σ) or steric effects (E_s), hydrophobicity (clog P), or localized hydrophobicity at the *p*-substituent (π) (see Supporting Information). Considering that the pK_a of benzoic acid is 4.2,¹⁶ it is hypothesized that the carboxylic acid of **21** is deprotonated upon addition to the cell culture media (pH ca. 7.4) and forms the carboxylate anion; thus the lipophilicity of the molecule is significantly reduced (see Supporting Information). This implies that the *p*-substituent may play an important role in the cytotoxicity of the *N*-alkylisatins, but the large variety of atoms that can be substituted at this position suggests that there is no highly specific binding interaction occurring in this region. Alternatively, carboxylate anion formation may reduce cell uptake and hence cytotoxicity.

The most potent compounds (i.e., IC₅₀ < 1 µM) determined from the initial cell line screen (Table 1) were subsequently tested against a panel of four additional adherent cancer cell lines (PC-3, MDA-MB-231, HCT-116, and A-375, Table 2) and one normal, non-transformed human cell line suspension (PBL, Figure 2). Of the nine compounds tested, four exhibited IC₅₀ values in the sub-micromolar range against at least one cell line (**17**, **19**, **23**, and **25**, Table 2). The colorectal carcinoma cell line (HCT-116) was the most susceptible to treatment, with compound **17** reducing the metabolic activity by 50% at a concentration of 0.53 µM. The MDA-MB-231 and A375 cell lines were moderately sensitive, while the prostate carcinoma cell line PC-3 was the least susceptible to treatment, as none of the compounds tested exhibited IC₅₀ values less than 1 µM. This differential effect is unlikely to be due to proliferative disparities, as all four cell lines have similar population doubling times. Furthermore, cancer cell line selectivity was observed for compound **19**, which exhibited >5 times more activity toward the lymphoma and leukemic cell lines than freshly

Table 2. Cytotoxicity of Selected *N*-Alkylisatins against Various Cancer Cell Lines As Determined by Dose Response Curves^a

compound	IC ₅₀ (µM) ^b			
	PC-3 ^c	MDA-MB-231 ^d	HCT-116 ^e	A375/ ^f
6	4.57	1.91	1.22	2.00
12	3.50	5.29	2.59	4.66
14	NT ^g	2.75	2.70	2.50
16	2.17	2.77	1.84	1.68
17	3.44	1.90	0.53	1.22
18	10.9	2.92	3.36	2.40
19	1.17	0.54	0.84	1.25
23	3.06	0.98	1.66	0.89
25	3.42	2.06	0.83	1.19

^a Sigmoidal dose response curves (variable slope) were generated using GraphPad Prism V. 4.02 (GraphPad Software Inc.). ^b Values are the mean of triplicates of at least two independent experiments. ^c PC-3: human prostate adenocarcinoma cell line. ^d MDA-MB-231: human mammary gland carcinoma (metastatic) cell line. ^e HCT-116: human colorectal carcinoma cell line. ^f A375: human malignant melanoma cell line. ^g NT = not tested.

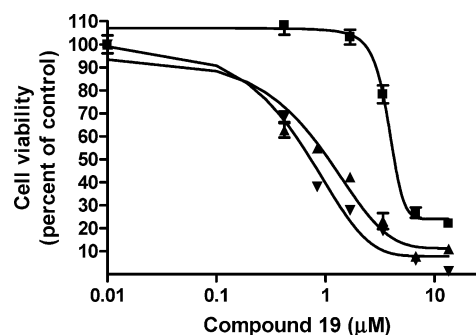


Figure 2. Cancer cell line selectivity. Different concentrations of 5,7-dibromo-*N*-(*p*-trifluoro-methylbenzyl)isatin (**19**) were incubated with either (■) freshly isolated, non-transformed, human peripheral blood lymphocytes (PBL), (▲) human monocytic-like, histiocytic lymphoma cells (U937), or (▼) a human leukemic T-cell line (Jurkat) for 24 h at 37 °C. Cells were then analyzed for a change in metabolic activity and expressed as percent viability in reference to the DMSO control. Each data point is a mean of triplicates \pm SE.

isolated, human PBLs (Figure 2). This is promising considering the lack of effective and nontoxic drugs available for the treatment of MDR lymphoid malignancies.^{17–19}

Mode of Action Investigations. Apoptosis and Cell Cycle Arrest. As it is known that several *N*-alkylindole derivatives trigger apoptosis⁸ and induce G2/M arrest,^{4,5,7} the effect of the most potent *N*-alkylisatins on the activation of the effector caspases-3 and -7 and cell cycle progression was investigated. Compound **19** was found to activate caspase-3 and -7 in a dose- (Figure 3A) and time-dependent manner (see Supporting Information) in Jurkat cells. At 3.3 µM, the activity of compound **19** was comparable to that of the staurosporine positive control. Unlike staurosporine, however, **19** exhibited a caspase activation trend in U937 cells similar to that seen in the Jurkat cell line, while only minimal caspase activity was observed in PBLs (Figure 3B). This compares closely with cytotoxicity data (Figure 2), whereby a decrease in the viability of cells correlates to an increase in the activation of effector caspases-3 and -7 and hence apoptosis. Such an effect was further supported by the appearance of fragmented nuclei in morphologically altered U937 cells after treatment with compound **18** (see Supporting Information). Furthermore, U937 cells treated with compounds **6** and **19** exhibited an increase in the accumulation of cells in G2/M, in comparison to vehicle control treated cells (Figure 4, panels G and H). This effect was both dose and time dependent, whereby mitotic arrest was most apparent at 0.5 µM after 24 h. At higher concentrations (i.e., 2 and 1 µM), cells treated with

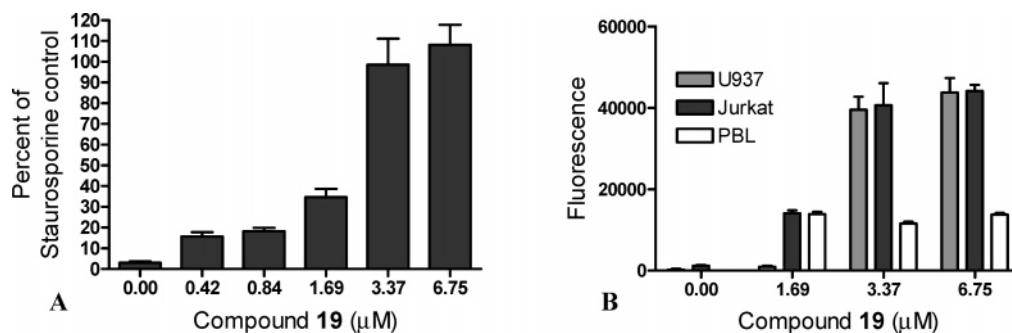


Figure 3. Activation of the effector caspases-3 and -7 in Jurkat, U937, and PBL cells after treatment with various *N*-alkylisatins. (A) Jurkat cells were exposed to increasing concentrations of 5,7-dibromo-*N*-(*p*-trifluoromethylbenzyl)isatin (**19**) for 5 h at 37 °C. Values were normalized to a staurosporine (positive control). (B) Jurkat, U937, and PBL cells were exposed to three concentrations of compound **19** for 5 h at 37 °C. In all cases, cells were then incubated with the caspase-3/7 reagent for 1 h at room temperature, and fluorescence was measured at an excitation wavelength of 485 and 520 nm emission. Data are means \pm SE of one representative experiment performed in triplicate.

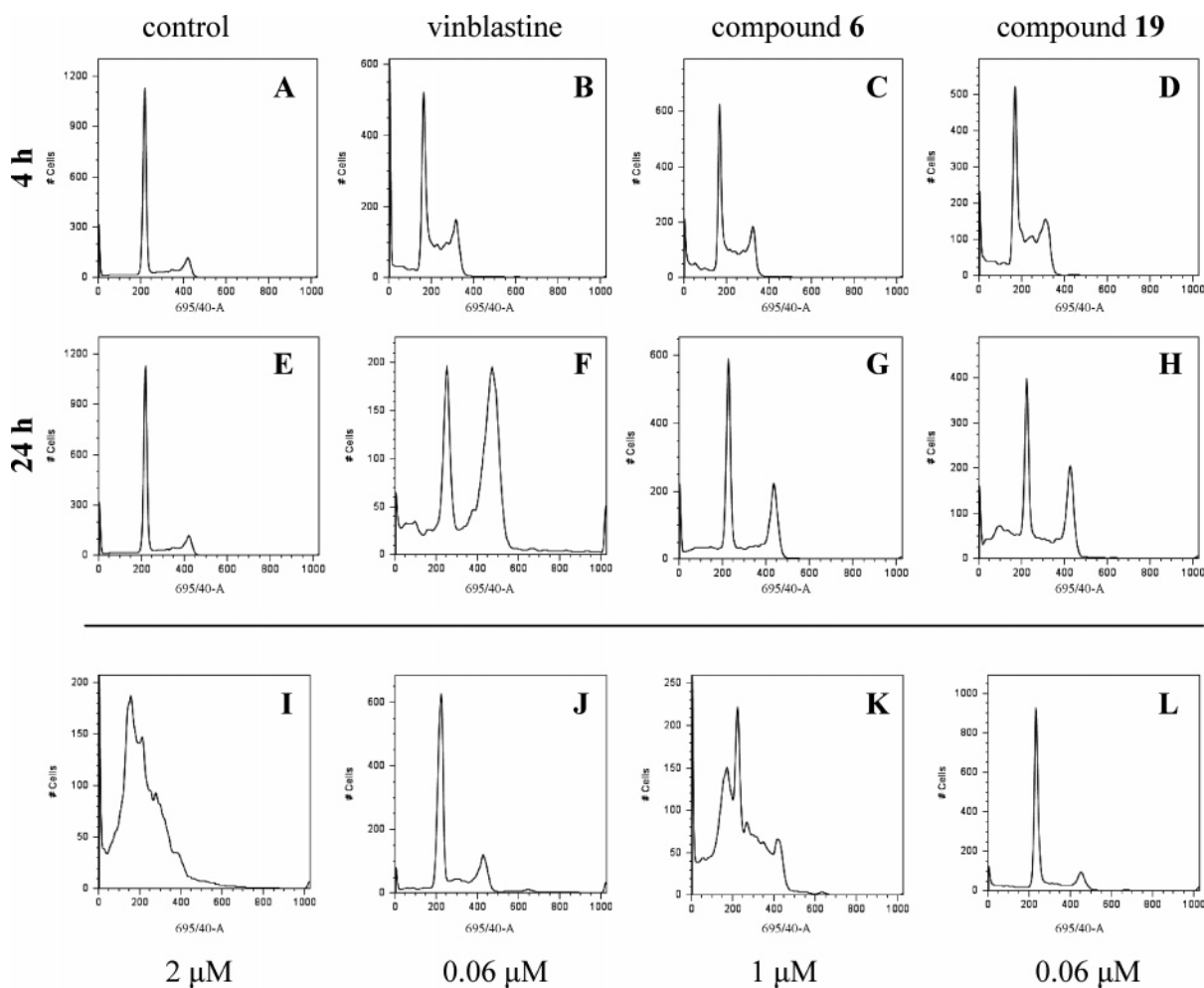


Figure 4. The effect of *N*-alkylisatins on the cell cycle. U937 cells were treated with either (A) and (E) DMSO vehicle control, (B) and (F) 0.5 μM vinblastine sulfate, (C) and (G) 0.5 μM 5,7-dibromo-*N*-(*p*-methylbenzyl)isatin (**6**), or (D) and (H) 0.5 μM 5,7-dibromo-*N*-(*p*-trifluoromethylbenzyl)isatin (**19**) for 4 h (upper panels) or 24 h (lower panels). Cells were then ethanol fixed, stained with propidium iodide, and analyzed for DNA distribution by FACS. Cell cycle arrest was additionally determined after treatment with high and low concentrations of compounds **6** (panels I and J) and **19** (panels K and L).

compounds **6** and **19** (respectively) showed an increase in S phase and sub-G1 peak distribution (Figure 4, panels I and K). Although not observed in vinblastine treated cells, this latter effect was consistent with the induction of apoptosis (Figure 3).

Effect on Lymphocyte Morphology. In addition to their potent cytotoxicity, various *N*-alkylisatins were also found to dramatically alter lymphocyte morphology (Figure 5). Within 5 h of incubation with less than 1 μM of various *N*-alkylisatins,

a sub-population of U937 cells developed an elongated formation as well as irregular membrane protrusions, of which the latter appeared to be consistent with an apoptotic response²⁰ (see Supporting Information). After 24 h, however, the elongated morphology was more pronounced (Figure 5). An analogous effect has also been reported for the benzylamide sulindac derivatives (1*Z*)-*N*-benzyl-5-fluoro-2-methyl-1-[(4-pyridyl)methyl]ene]-1*H*-indene-3-acetamide hydrochloride (CP461) and (1*Z*)-*N*-benzyl-5-fluoro-2-methyl-1-[[4-(3,4,5-trimethoxyphenyl)-

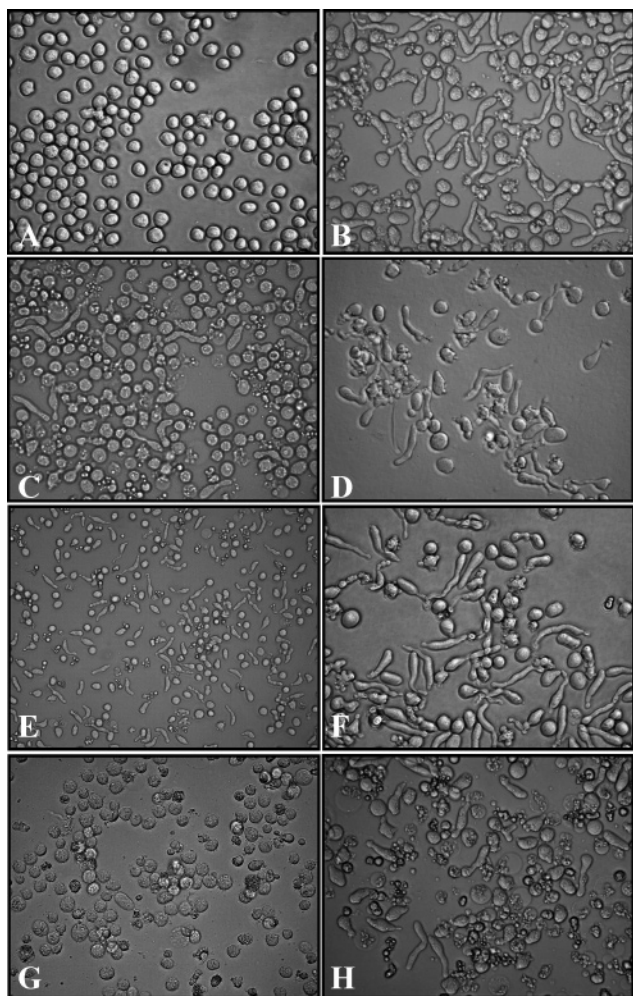


Figure 5. Morphological effects of various *N*-alkylisatins and commercial anticancer agents on U937 cells. Cells (1.0×10^4) were incubated with either (A) DMSO vehicle control, (B) 5,7-dibromo-*N*-(cinnamyl)isatin (**24**), (C) vinblastine sulfate salt, (D) 5,7-dibromo-*N*-(isopentyl)isatin (**4**), (E) paclitaxel, (F) 5,7-dibromo-*N*-(*p*-iodobenzyl)isatin (**18**), (G) 5-fluorouracil, or (H) 5,7-dibromo-*N*-(*p*-*tert*-butylbenzyl)isatin (**23**) all at $0.39 \mu\text{g/mL}$ for 24 h. Images were obtained by brightfield microscopy on an inverted light microscope using a Leica DC500 12-megapixel high-performance FireWire camera system. Images (panels A–D and F–H) were viewed at $1000\times$ magnification, and image E was viewed at $400\times$ magnification.

methylene]}-1*H*-indene-3-acetamide (CP2-48), whereby examination of WSU-CLL cells after an 18 h treatment revealed a marked affect on cell shape.²¹ Interestingly, the structurally similar parent compounds, sulindac sulfide and sulindac sulfone, currently being studied as chemo-preventatives in patients with familial adenomatous polyposis (FAP),²² did not.

A change in leukemic T-cell morphology was also noted after treatment with compound **18** (see Supporting Information) but was not as obvious as that observed in the monocytic cell line. Morphological alterations were also seen in vinblastine (Figure 5, panel C) and paclitaxel (Figure 5, panel E) treated cells, but not in cells treated with 5-fluorouracil (Figure 5, panel G) or staurosporine (see Supporting Information), suggesting that *N*-alkylisatins may either disrupt or stabilize microtubules in a fashion similar to the *Vinca* alkaloids²³ or taxanes.²⁴

Effects on Tubulin Polymerization and Microtubule Formation. The indolic heterocyclic nucleus is central to a large number of tubulin polymerization inhibitors.^{7,25–27} Isatins are oxidized derivatives of an indolic moiety, and considering the broad range of *N*-alkylisatins that showed potent cell-based

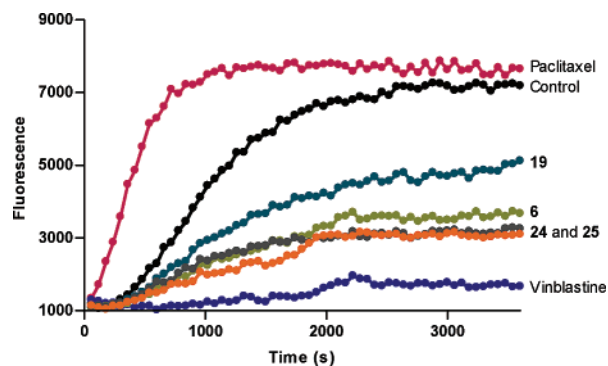


Figure 6. The effect of various *N*-alkylisatins and commercial anticancer agents on tubulin polymerization as determined in the *in vitro* microtubule polymerization assay. Purified bovine neuronal tubulin was used to assay for microtubule formation in the presence of either: black circle, vehicle control; red circle, paclitaxel $10 \mu\text{M}$; dark blue circle, vinblastine sulfate salt $10 \mu\text{M}$; green circle, 5,7-dibromo-*N*-(*p*-methylbenzyl)isatin (**6**) $10 \mu\text{M}$; teal circle, 5,7-dibromo-*N*-(*p*-trifluoromethylbenzyl) isatin (**19**) $10 \mu\text{M}$; dark brown circle, 5,7-dibromo-*N*-(cinnamyl)isatin (**24**) $10 \mu\text{M}$; or orange circle, 5,7-dibromo-*N*-(*p*-phenylbenzyl)isatin (**25**) $10 \mu\text{M}$ at 37°C . A shift of the curve to the left or right of the control is indicative of either an increase or a decrease, respectively, in the rate of tubulin polymerization. Changes in fluorescence were measured at an excitation wavelength of $360 \pm 10 \text{ nm}$, and the fluorescence was collected at $440 \pm 10 \text{ nm}$. Data points are the means of duplicate experiments.

activity and morphological change in this study, compounds **6**, **19**, **24**, and **25** were chosen as representative molecules to further investigate their ability to alter tubulin polymerization *in vitro*. As expected, the potent microtubule stabilizing agent paclitaxel resulted in a dramatic increase in the rate of tubulin polymerization at $10 \mu\text{M}$, in comparison to the vehicle control, while vinblastine strongly inhibited microtubule formation at the same concentration (Figure 6). This was greater than the effect seen at $3 \mu\text{M}$ (see Supporting Information), indicating that the rate of microtubule stabilization or destabilization is dose-dependent. The *N*-alkylisatins **6**, **19**, **24**, and **25** also strongly inhibited the rate of microtubule polymerization at $10 \mu\text{M}$, albeit not as potently as vinblastine (Figure 6). This effect appeared to be independent of the nature of the *p*-substituent and size of the benzene carbon linker, because compounds **6**, **24**, and **25** all inhibited microtubule polymerization at a similar rate. By comparison, compound **19** was slightly less active, but considering **19** shows broad cell-line cytotoxicity (Tables 1 and 2), this suggests that cell death induced by direct microtubule destabilization may not be its primary mechanism of action.

The role **19** played in the alteration of microtubule organization in comparison to DMSO and vinblastine treated lymphoma cells was further investigated by fluorescence microscopy, using fluorescently labeled paclitaxel. Compound **19** induced the accumulation of cells with fragmented microtubules, abnormal mitotic spindles, and reduced cell-associated fluorescence (Figure 7, panels B–D). Conversely, cells treated with vinblastine revealed highly fragmented microtubules at both high (Figure 7, panel E) and low (Figure 7, panel F) concentrations. Compound **19** and *N*-alkylisatins in general are a collection of low molecular weight compounds that show no structural similarities to the *Vinca* alkaloids, and while binding at the same site as these alkaloids may still be a possibility, interaction at another tubulin site is also feasible. Recently, a methylindole-2-carboxylate derivative was reported to adopt an orientation similar to that of an analogue, *N*-deacetyl-*N*-(2-mercaptoacetyl)-colchicine (DAMA-colchicine) of colchicine (**26**), when docked into the colchicine binding site of tubulin.²⁸ Similarly, A-432411

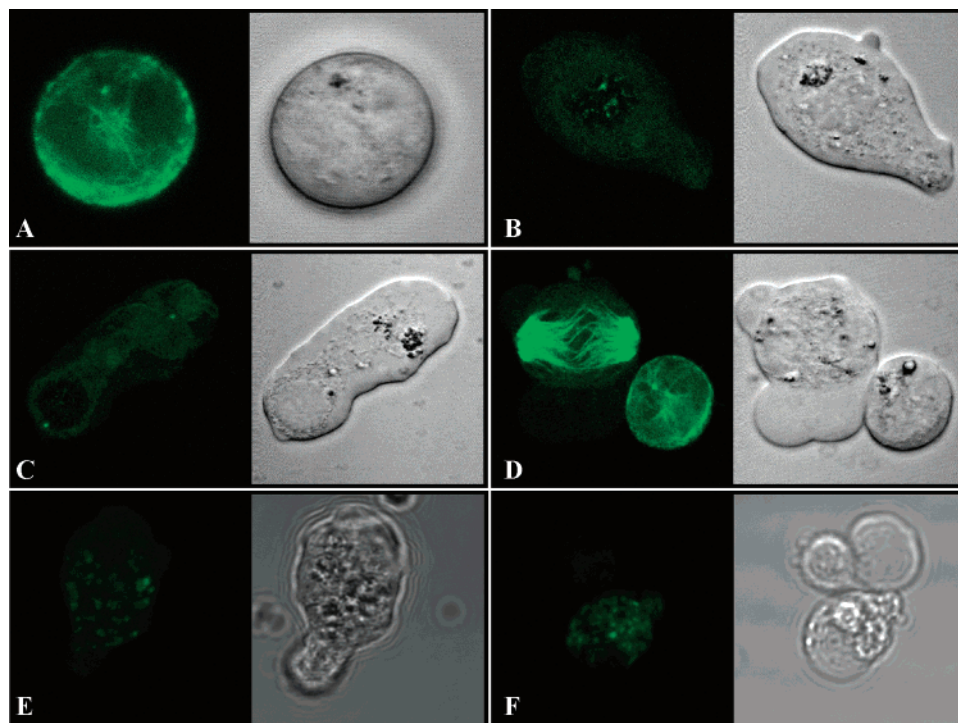


Figure 7. The effect of 5,7-dibromo-*N*-(*p*-trifluoromethylbenzyl) isatin (**19**) on the stability of microtubules in U937 cells. Treatment of cells with (A) DMSO was used as the control. Cells were exposed to either (B)–(D) 0.78 $\mu\text{g/mL}$ (1.7 μM) of compound **19** or (E) 0.78 $\mu\text{g/mL}$ (0.9 μM) or (F) 0.20 $\mu\text{g/mL}$ (0.2 μM) of the commercial anticancer agent vinblastine sulfate salt for 24 h. Microtubules were then visualized by direct fluorescence microscopy after incubation for 30 min with fluorescently labeled paclitaxel.

(**27**) was found to compete strongly with [^3H]colchicine (IC_{50} 0.13 μM) in a competition-binding scintillation proximity assay.⁶ Conversely, the indole derivative **1** did not compete for the binding of either radiolabeled vincristine or colchicine to tubulin.⁷ This suggests that **1** may bind to a novel binding site on tubulin and induce inhibition of polymerization. Because it is known that there are three major, well-characterized binding sites on tubulin,^{23,29,30} it would be of interest to conduct future competitive binding studies, as well as molecular modeling and docking studies, to verify the exact binding interactions between the various *N*-alkylisatins (from this study) and tubulin and correlate this with SAR data.

Alternatively, it is also possible that *N*-alkylisatin-induced microtubule disassembly is a secondary phenomenon, despite some characteristics resembling those induced by the destabilizing agent vinblastine. For example, treatment of cells with the microtubule-dissociating agent nocodazole (**28**) has been reported to result in Raf1 activation by Pak1, a kinase downstream of the small GTPases Rac/Cdc42.³¹ Activated Rac and Cdc42 induce cell shape changes at the plasma membrane by formation of multimolecular focal complexes as well as lamellipodia and filopodia.³² It may therefore be of interest in future studies to also determine whether various *N*-alkylisatins activate the Rac/Cdc42/Pak1/Raf1 signaling pathway.

Conclusions

N-Alkyl- and arylalkylisatins, in particular compounds **6**, **12**, **14**, **16**, **17**, **18**, **19**, **23**, and **25**, are novel synthetic anticancer agents with potent cytotoxicity in vitro, some of which show >22 times selectivity for leukemic cells over the MCF-7, epithelial breast adenocarcinoma. Compound **19** also exerted significant anticancer activity on a broad range of cancer cell lines including leukemic, lymphoma, colorectal, breast, prostate, and melanoma cells and was found, together with the most active compound, **6**, to destabilize microtubules in tumor cells as well

as in a cell-free system. The potent cytotoxicity displayed by the various *N*-alkylisatins as compared to the commercial anticancer agents, vinblastine and taxol, together with the possibility of binding to a novel site on tubulin, suggest that these compounds may be beneficial in the treatment of anti-mitotic drug-resistant tumors in the future.

Experimental Section

General Synthesis and Experimental Methods. The desired isatin starting materials were either purchased or synthesized using previously reported methods.³ 4-Bromoisatin, 6-bromoisatin, and 7-bromoisatin were obtained from Butt Park Ltd. (U.K.). All other chemicals were purchased from the major vendors. Reactions were carried out using dried glassware and under an atmosphere of nitrogen. All solvents were AR grade except dichloromethane (DCM), which was LR grade and distilled before use. Reactions were monitored using thin layer chromatography (TLC) on aluminum backed precoated silica gel 60 F₂₅₄ plates (E. Merck). The *N*-alkylisatins were highly colored and would usually be clearly seen on a TLC plate; colorless compounds were detected using UV light and/or iodine vapor. Flash chromatography³³ was carried out using silica gel 60 (230–400 mesh, E. Merck) with the solvent system indicated in the individual procedures. All solvent ratios are quoted as vol/vol. ^1H and ^{13}C NMR spectra of compounds **2**–**25** were acquired at 300 and 75 MHz, respectively, on a Varian Unity-300 spectrometer and 500 and 126 MHz, respectively, on a Varian Inova-500 spectrometer with a probe temperature of 298 K. The NMR spectra are referenced to the residual solvent peak in the solvent stated in the individual procedures. Hydrogen and carbon assignments were made using standard NOE, APT, DEPT, gCOSY, gHSQC, and gHMBC spectroscopic techniques. Low-resolution EI mass spectra (LREI-MS) were determined on a Shimadzu QP5050 spectrometer. High-resolution EI mass spectra (HREI-MS) were determined on VG Autospec spectrometer operating at 70 eV with a source temperature of 250 $^{\circ}\text{C}$ and were referenced with PFK. Melting points were determined on a Reichert melting point apparatus and are uncorrected.

General Method for the Alkylation of Isatins. The appropriate isatin (~200 mg, 1 equiv) was taken up in anhydrous DMF (1 mL per 0.1 mmol of isatin) and cooled on ice with stirring. Solid K_2CO_3 (1.2 equiv) or CS_2CO_3 (1.2 equiv) was added in one portion, and the dark colored suspension was brought to room temperature and stirred for a further 1 h. The appropriate alkyl chloride (1.1 equiv for compounds **7–12** and **16**) or bromide (1.1 equiv for all other relevant compounds) and KI (0.2 equiv) were added, and the reaction mixture was stirred at 80 °C for 5–24 h, until the isatin starting material had been consumed (TLC). The reaction mixture was poured into HCl (0.5 M, 50 mL) and extracted with ethyl acetate (1 × 50 mL). The ethyl acetate layer was washed with brine and dried over $MgSO_4$. The solvent was removed, and the crude product was purified via flash column chromatography using isocratic elution with CH_2Cl_2 unless otherwise stated.

***N*-Allyl-5,7-dibromoisatin (2).** The product was a bright red solid (102 mg, 45%), mp 103–105 °C (lit.³⁴ 98–100 °C), R_f 0.45 (CH_2Cl_2 , silica). 1H NMR ($CDCl_3$, 500 MHz) δ 4.79 (d, $J = 5$ Hz, 2H, CH_2), 5.23 (d, $J = 17$ Hz, 1H, $CH_{cis}H_{trans}$), 5.26 (d, $J = 10$ Hz, 1H, $CH_{cis}H_{trans}$), 5.96 (ddt, $J = 5, 10, 17$ Hz, 1H, CH), 7.70 (d, $J = 2$ Hz, 1H, H4), 7.86 (d, $J = 2$ Hz, 1H, H6). ^{13}C NMR ($CDCl_3$, 126 MHz) δ 43.1, 104.9, 116.8, 117.6, 121.1, 127.3, 131.4, 145.1, 146.6, 157.7, 181.2. The quoted 1H and ^{13}C NMR spectral data were in agreement with published values.³⁴ LREI-MS m/z 343/345/347 ($[M]^+ / [M + 2]^+ / [M + 4]^+$).

5,7-Dibromo-*N*-(*p*-methylbenzyl)isatin (6) (CAS No. 620932-72-1). The product was a bright red solid (252 mg, 93%), mp 121–123 °C, R_f 0.61 (CH_2Cl_2 , silica). 1H NMR ($CDCl_3$, 500 MHz) δ 2.30 (s, 3H, CH_3), 5.34 (s, 2H, $H1'$), 7.11 (d, $J = 8$ Hz, 2H, phenyl ArH), 7.13 (d, $J = 8$ Hz, 2H, phenyl ArH), 7.66 (d, $J = 2$ Hz, 1H, isatin ArH), 7.77 (d, $J = 2$ Hz, 1H, isatin ArH). ^{13}C NMR ($CDCl_3$, 126 MHz) δ 21.0, 44.3, 105.1, 116.9, 121.3, 126.3, 127.3, 129.3, 132.5, 137.3, 145.1, 146.6, 158.2, 181.2. LREI-MS m/z 407/409/411 ($[M]^+ / [M + 2]^+ / [M + 4]^+$). HREI-MS m/z calcd for $[M]^+ C_{16}H_{11}^{79}Br_2NO_2$, 406.9157; found, 406.9175.

4-[(5,7-Dibromo-2,3-dihydro-2,3-dioxo-1*H*-indol-1-yl)methyl]benzoic Acid (21). The methyl ester **22** (70 mg, 0.15 mmol) was dissolved in a mixture of concentrated HCl (8 mL), glacial acetic acid (8 mL), and water (2 mL) and stirred at reflux for 1.5 h. The reaction mixture was poured onto ice (100 mL) and extracted with ethyl acetate (2 × 100 mL), and the combined ethyl acetate layers were washed with brine and dried over $MgSO_4$. The solvent was removed to yield a bright orange solid. The solid was suspended in CH_2Cl_2 (20 mL) and then filtered, and the resulting solid was washed with CH_2Cl_2 to remove any trace of starting material. The product **21** was a bright red-orange solid (59 mg, 90%), mp >250 °C, R_f 0.13 (9:1 CH_2Cl_2 :MeOH, silica). 1H NMR (DMSO- d_6 , 500 MHz) δ 5.30 (s, 2H, CH_2), 7.50 (d, $J = 8$ Hz, 2H, ArH), 7.79 (d, $J = 2$ Hz, 1H, isatin ArH), 7.88 (d, $J = 8$ Hz, 2H, ArH), 7.98 (d, $J = 2$ Hz, 1H, isatin ArH), 12.80 (br s, 1H, OH). ^{13}C NMR (DMSO- d_6 , 126 MHz) δ 44.9, 104.8, 116.4, 123.5, 127.0, 130.1, 130.3, 143.0, 143.9, 146.8, 159.8, 167.8, 181.2. LREI-MS m/z 437/439/451 ($[M]^+ / [M + 2]^+ / [M + 4]^+$). HREI-MS m/z calcd for $[M + 2]^+ C_{16}H_9^{79}Br^{81}BrNO_4$, 438.8878; found, 438.8880.

Materials and Reagents for Cell Culture and Bioassays. The culture medium RPMI-1640 was purchased from Gibco (Invitrogen Life Technologies, NSW, Australia). Fetal calf serum (FCS) was obtained from MultiSer (ThermoTrace, Vic., Australia). Sodium bicarbonate was purchased from Univar Analytical Reagents (Ajax Chemicals, Australia). Trypsin–EDTA solution was purchased from Sigma–Aldrich (MO). Lymphoprep was purchased from Pharmacia Biotech, Australia. The CellTiter 96 AQueous One Solution Cell Proliferation Assay and Apo-ONE Homogeneous Caspase-3/7 Assay were purchased from Promega Co. (Madison, WI). Tubulin Tracker Green Reagent (fluorescently labeled paclitaxel) was obtained from Molecular Probes (Invitrogen Aust. Pty Ltd., Australia), and the Tubulin Polymerization Assay was from Cytoskeleton Inc. (Jomar Diagnostics, Australia). The Diff-Quik staining kit was purchased from Lab Aids (Sydney, NSW Australia), and propidium iodide was from Sigma–Aldrich (St. Louis, MO). Light and fluorescence microscopy images were obtained using a

Leica DC500 12-megapixel high-performance FireWire camera system (Leica Microsystems, AG, Germany) and the Leica IM50 image manager software (Leica Microsystems AG, Heerbrugg, Germany).

Cell Lines and Culture Conditions. The human lymphoma (U937), leukemic (Jurkat), breast (MDA-MB-231 and MCF-7), prostate (PC-3), and colorectal (HCT-116) carcinoma cell lines as well as the melanoma (A375) cell line were all obtained from American Type Culture Collection (ATCC, VA) distributed by Cryosite, NSW, Australia. Cell lines were routinely cultured at 37 °C in a Heracell incubator (Kendo Laboratory Products, Langensfeld, Germany) in 95% humidified atmosphere, containing 5% CO_2 . Cells were grown in culture media (10.4 g/L RPMI-1640 with 2 mM L-glutamine and 2 g/L $NaHCO_3$) supplemented with 5% (v/v) fetal calf serum (FCS), and routinely passaged at confluency for up to 20 passages. Adherent cell lines were detached using sterile trypsin–EDTA, washed with culture media, and centrifuged at 1500 rpm (514g) for 5 min at room temperature (RT) before reseeding. All cell experiments were performed using cells in exponential growth, cultured 48 h before without change of media. Adherent cells were detached prior to experiments with sterile phosphate-buffered saline (PBS) containing 5 mM EDTA (pH 7.4), and cells were then centrifuged at 1500 rpm (514g) for 5 min at RT. Human peripheral blood lymphocytes (PBL) were prepared fresh, on the day of use, by density centrifugation. Briefly, Lymphoprep (7 mL) was carefully layered beneath fresh, human, peripheral blood (10 mL) that had been diluted 1:2 in PBS (pH 7.4). The preparation was then centrifuged (Heraeus megafuge) at 1800 rpm (800g) for 20 min at RT. After centrifugation, the top, diluted, plasma layer was carefully removed and discarded. The opaque layer, at the interface, containing peripheral blood lymphocytes (PBL) was collected and placed into a sterile tube. Collected cells were then washed twice with PBS by centrifugation at 1800 rpm (800g) for 30 min at RT, and the supernatant was discarded. Pelleted cells were finally resuspended in 2 mL of complete media RPMI-1640 supplemented with 5% FCS. Cell viability and cell number were assessed by the Trypan blue exclusion method, and viable cells were counted with the aid of a hemocytometer.

Cell Viability (MTS) Assay. Cytotoxicity of the isatin derivatives on various cancer and non-transformed cell lines was determined using the CellTiter 96 AQueous One Solution Cell Proliferation Assay (MTS), in 96-well microplates, as described previously.³⁵ Test compounds were incubated with different cell lines at increasing concentrations ranging from 0 to 100 $\mu g/mL$ for 24 h (unless stated otherwise) prior to the addition of MTS reagent. Cytotoxic activity was then determined spectrophotometrically at 490 nm. Results for each compound are reported as the concentration (μM) required to inhibit the metabolic activity of 50% of the cell population (IC_{50}) in comparison to vehicle-treated (DMSO) control cells. These values were calculated from logarithmic sigmoidal dose response curves using the variable slope parameter, generated from GraphPad Prism V. 4.02 software (GraphPad Software Inc.).

Caspase-3/7 Assay. The activation of effector caspases-3 and -7 was determined in Jurkat, U937, and PBL cells after incubation with test compound or 2 μM staurosporine (positive control) using the Apo-ONE Homogeneous Caspase-3/7 Assay kit. The assay was carried out according to the method described previously.³

Cell Cycle Analysis by Flow Cytometry. Flow cytometry analysis of cellular DNA content was performed using a modification to the method described previously.⁶ Briefly, cells (2.0×10^4) were harvested by centrifugation at 1500 rpm (514g) for 5 min and fixed with ice-cold ethanol (70%) for 30 min to overnight at –20 °C. The ethanol was then removed by centrifugation, and cells were stained with PI master mix (100 $\mu g/mL$ RNase A, 40 $\mu g/mL$ PI, and PBS pH 7.4) for 30 min at 37 °C. DNA content was then measured using a Becton Dickinson BD LSR II FACSsort flow cytometer (BD Biosciences, USA), and the proportion of cells in G0/G1, S, and G2/M phases of cell cycle was calculated on the

basis of DNA distribution histograms using FlowJo software (V7.1, Tree Star Inc., USA).

Effect on Tubulin Polymerization. (a) Live Cell Staining. U937 cells (2.2×10^5 cells/mL, 90 μ L) were seeded into the wells of a 96-well microtiter plate and incubated for 24 h (37 °C, 95% humidity, 5% CO₂) prior to the addition of test compound. Compound **19** (10 μ L) was then added to the cells at a concentration that induced the greatest amount of morphological change (as determined from light microscopy) and incubated for a further 24 h. Control samples were also prepared by incubating cells with either 2 μ M vinblastine sulfate salt (positive control) or 2.5% DMSO (negative control) for 24 h. Cells were then stained with freshly prepared TubulinTracker Green reagent at a final concentration of 250 nM for 0.5 h (37 °C, 95% humidity, 5% CO₂) as per the manufacturer's instructions. Stained cells were washed once with Dulbecco's PBS, and fluorescence was visualized by confocal microscopy. Confocal laser scanning microscopy images were acquired using a Leica TCS SP system and the UV 63 \times 1.32 N.A. oil PALPO immersion objective lens (Leica, Heidelberg, Germany). Cells were excited using the 488 nm spectral line of the Argon ion laser, and fluorescence was measured at 500–540 nm.

(b) Tubulin Polymerization Assay. Compounds were tested for their anti-mitotic ability in reference to vinblastine sulfate and paclitaxel positive controls in a fluorescence-based Tubulin Polymerization Assay.³⁶ Briefly, 50 μ L of tubulin reaction mix (2 mg/mL purified bovine brain tubulin in 80 mM PIPES pH 6.9, 2.0 mM MgCl₂, 0.5 mM EGTA, 1.0 mM GTP, and 20% glycerol) was added to duplicate wells of a half area 96-well black plate containing 5 μ L of either vehicle control, paclitaxel, vinblastine sulfate, or compounds **6**, **19**, **24**, and **25** all at a final concentration of 3 or 10 μ M. The rate of polymerization was followed for 1 h at 37 °C using an excitation wavelength of 360 ± 10 nm, and the fluorescence was collected at 440 ± 10 nm.

Acknowledgment. We are grateful to the University of Wollongong for support through the Institute for Biomolecular Science (IBS), a URC Small Grant, a University Cancer Research Grant, and a UPA student scholarship for K.L.V. We also thank Dr. K. Benkendorff (Flinders University, South Australia) for support, and the Illawarra Cancer Carers Inc., Kiama, Minnamurra, and Gerringong Sunrise Rotary, The Robert East Memorial Fund, Prof. P. Clingan, and other private donors for funding assistance. Assoc. Prof. M. Ranson is a recipient of a Cancer Institute NSW Fellowship award.

Supporting Information Available: Spectroscopic (¹H NMR, ¹³C NMR, and MS) data for compounds **3–5**, **7–20**, and **22–25**, HPLC purity data for compounds **2–25**, physicochemical properties of selected *N*-alkylisatins, activation of the effector caspases-3 and -7 in Jurkat cells, morphological evaluation of nuclei stained with Diff Quik, morphological effects of compounds **24**, **18**, and staurosporine on U937 or Jurkat cells, and the effect of compound **19** on tubulin polymerization. This material is available free of charge via the Internet at <http://pubs.acs.org>.

References

- Pandeya, S. N.; Smitha, S.; Jyoti, M.; Sridhar, S. K. Biological activities of isatin and its derivatives. *Acta Pharm.* **2005**, *55*, 27–46.
- Cane, A.; Tournaire, M. C.; Barritault, D.; Crumeyrolle-Arias, M. The endogenous oxindoles 5-hydroxyoxindole and isatin are anti-proliferative and proapoptotic. *Biochem. Biophys. Res. Commun.* **2000**, *276*, 379–384.
- Vine, K. L.; Locke, J. M.; Ranson, M.; Benkendorff, K.; Pyne, S. G.; Bremner, J. B. In vitro cytotoxicity evaluation of some substituted isatin derivatives. *Bioorg. Med. Chem.* **2007**, *15*, 931–938.
- Bramson, H. N.; Corona, J.; Davis, S. T.; Dickerson, S. H.; Edelman, M. Oxindole-based inhibitors of cyclin-dependent kinase 2 (CDK2): design, synthesis, enzymatic activities, and X-ray crystallographic analysis. *J. Med. Chem.* **2001**, *44*, 4339–4358.
- Andreani, A.; Granaiola, M.; Leoni, A.; Locatelli, A.; Morigi, R.; Rambaldi, M.; Garaliene, V.; Welsh, W.; Arora, S.; Farruggia, G.; Masotti, L. Antitumor activity of new substituted 3-(5-imidazo[2,1-b]thiazolylmethylene)-2-indolinones and study of their effect on the cell cycle. *J. Med. Chem.* **2005**, *48*, 5604–5607.
- Chen, Z.; Merta, P. J.; Lin, N. H.; Tahir, S. K.; Kovar, P.; Sham, H. L.; Zhang, H. A-432411, a novel indolinone compound that disrupts spindle pole formation and inhibits human cancer cell growth. *Mol. Cancer Ther.* **2005**, *4*, 562–568.
- Bacher, G.; Nickel, B.; Emig, P.; Vanhoefler, U.; Seeber, S.; Shandra, A.; Klenner, T.; Beckers, T. D-24851, a novel synthetic microtubule inhibitor, exerts curative antitumoral activity in vivo, shows efficacy toward multidrug-resistant tumor cells, and lacks neurotoxicity. *Cancer Res.* **2001**, *61*, 392–399.
- Nguyen, J. T.; Wells, J. A. Direct activation of the apoptosis machinery as a mechanism to target cancer cells. *Proc. Natl. Acad. Sci. U.S.A.* **2003**, *100*, 7533–7538.
- Liu, Y.; Lashuel, H. A.; Choi, S.; Xing, X.; Case, A.; Ni, J.; Yeh, L. A.; Cuny, G. D.; Stein, R. L.; Lansbury, P. T., Jr. Discovery of inhibitors that elucidate the role of UCH-L1 activity in the H1299 lung cancer cell line. *Chem. Biol.* **2003**, *10*, 837–846.
- Lee, J. W.; Moon, M. J.; Min, H. Y.; Chung, H. J.; Park, E. J.; Park, H. J.; Hong, J. Y.; Kim, Y. C.; Lee, S. K. Induction of apoptosis by a novel indirubin-5-nitro-3'-monoxime, a CDK inhibitor, in human lung cancer cells. *Bioorg. Med. Chem. Lett.* **2005**, *15*, 3948–3952.
- Torres, J. C.; Pinto, A. C.; Garden, S. J. Application of a catalytic palladium biaryl synthesis reaction via C-H functionalization, to the total synthesis of Amaryllidaceae alkaloids. *Tetrahedron* **2004**, *60*, 9889–9900.
- Piche, A.; Grim, J.; Rancourt, C.; Gomez-Navarro, J.; Reed, J. C.; Curiel, D. T. Modulation of Bcl-2 protein levels by an intracellular anti-Bcl-2 single-chain antibody increases drug-induced cytotoxicity in the breast cancer cell line MCF-7. *Cancer Res.* **1998**, *58*, 2134–2140.
- Sakakura, C.; Sweeney, E. A.; Shirahama, T.; Hakomori, S.; Igarashi, Y. Suppression of bcl-2 gene expression by sphingosine in the apoptosis of human leukemic HL-60 cells during phorbol ester-induced terminal differentiation. *FEBS Lett.* **1996**, *379*, 177–180.
- Zhang, B.; Zhang, D.; Ren, H. Resistance of Bcl-2 adenovirus vector to HepG(2) cell apoptosis induced by ethanol. *Zhonghua Gan Zang Bing Za Zhi* **2000**, *8*, 215–217.
- Campos, L.; Rouault, J. P.; Sabido, O.; Oriol, P.; Roubi, N.; Vasselon, C.; Archimbaud, E.; Magaud, J. P.; Guyotat, D. High expression of bcl-2 protein in acute myeloid leukemia cells is associated with poor response to chemotherapy. *Blood* **1993**, *81*, 3091–3096.
- The Merck Index: An Encyclopedia of Chemicals, Drugs, and Biologicals*, 14th ed.; O'Neil, M. J. (Editor), Heckelman, P. E. (Senior Associate Editor), Koch, C. B. (Associate Editor), Roman, K. J. (Assistant Editor); Merck and Co., Inc.: Whitehouse Station, NJ, 2006; p 2564.
- Drenou, B.; Lamy, T.; Amiot, L.; Fardel, O.; Caulet-Maugendre, S.; Sasportes, M.; Diebold, J.; Le Prise, P. Y.; Fauchet, R. CD3- CD56+ non-Hodgkin's lymphomas with an aggressive behavior related to multidrug resistance. *Blood* **1997**, *89*, 2966–2974.
- Newcomb, E. W. P53 gene mutations in lymphoid diseases and their possible relevance to drug resistance. *Leuk. Lymphoma* **1995**, *17*, 211–221.
- Nooter, K.; Sonneveld, P. Multidrug resistance (MDR) genes in haematological malignancies. *Cytotechnology* **1993**, *12*, 213–230.
- Kroemer, G.; Dallaporta, B.; Resche-Rigon, M. The mitochondrial death/life regulator in apoptosis and necrosis. *Annu. Rev. Physiol.* **1998**, *60*, 619–642.
- Moon, E. Y.; Lerner, A. Benzylamide sulindac analogues induce changes in cell shape, loss of microtubules and G(2)-M arrest in a chronic lymphocytic leukemia (CLL) cell line and apoptosis in primary CLL cells. *Cancer Res.* **2002**, *62*, 5711–5719.
- van Stolk, R.; Stoner, G.; Hayton, W. L.; Chan, K.; DeYoung, B.; Kresty, L.; Kemmenoe, B. H.; Elson, P.; Rybicki, L.; Church, J.; Provencher, K.; McLain, D.; Hawk, E.; Fryer, B.; Kelloff, G.; Ganapathi, R.; Budd, G. T. Phase I trial of exisulind (sulindac sulfone, FGN-1) as a chemopreventive agent in patients with familial adenomatous polyposis. *Clin. Cancer Res.* **2000**, *6*, 78–89.
- Rai, S. S.; Wolff, J. Localization of the vinblastine-binding site on beta-tubulin. *J. Biol. Chem.* **1996**, *271*, 14707–14711.
- Schiff, P. B.; Fant, J.; Horwitz, S. B. Promotion of microtubule assembly in vitro by taxol. *Nature* **1979**, *277*, 665–667.
- Gastpar, R.; Goldbrunner, M.; Marko, D.; von Angerer, E. Methoxy-substituted 3-formyl-2-phenylindoles inhibit tubulin polymerization. *J. Med. Chem.* **1998**, *41*, 4965–4972.
- Beckers, T.; Mahboobi, S. Natural, semisynthetic and synthetic microtubule inhibitors for cancer therapy. *Drugs Future* **2003**, *28*, 767–785.

- (27) Brancale, A.; Silvestri, R. Indole, a core nucleus for potent inhibitors of tubulin polymerization. *Med. Res. Rev.* **2007**, *27*, 209–238.
- (28) De Martino, G.; Edler, M. C.; La Regina, G.; Coluccia, A.; Barbera, M. C.; Barrow, D.; Nicholson, R. I.; Chiosis, G.; Brancale, A.; Hamel, E.; Artico, M.; Silvestri, R. New arylthioindoles: potent inhibitors of tubulin polymerization. 2. Structure-activity relationships and molecular modeling studies. *J. Med. Chem.* **2006**, *49*, 947–954.
- (29) Uppuluri, S.; Knipling, L.; Sackett, D. L.; Wolff, J. Localization of the colchicine-binding site of tubulin. *Proc. Natl. Acad. Sci. U.S.A.* **1993**, *90*, 11598–11602.
- (30) Rao, S.; Orr, G. A.; Chaudhary, A. G.; Kingston, D. G.; Horwitz, S. B. Characterization of the taxol binding site on the microtubule. 2-(m-Azidobenzoyl)taxol photolabels a peptide (amino acids 217–231) of beta-tubulin. *J. Biol. Chem.* **1995**, *270*, 20235–20238.
- (31) Zang, M.; Waelde, C. A.; Xiang, X.; Rana, A.; Wen, R.; Luo, Z. Microtubule integrity regulates Pak leading to Ras-independent activation of Raf-1, insights into mechanisms of Raf-1 activation. *J. Biol. Chem.* **2001**, *276*, 25157–25165.
- (32) Nobes, C. D.; Hall, A. Rho, rac and cdc42 GTPases: regulators of actin structures, cell adhesion and motility. *Biochem. Soc. Trans.* **1995**, *23*, 456–459.
- (33) Still, W. C.; Kahn, M.; Mitra, A. Rapid chromatographic technique for preparative separations with moderate resolution. *J. Org. Chem.* **1978**, *43*, 2923–2925.
- (34) Garden, S. J.; Torres, J. C.; da Silva, L. E.; Pinto, A. C. A convenient methodology for the N-alkylation of isatin compounds. *Synth. Commun.* **1998**, *28*, 1679–1689.
- (35) Cory, A. H.; Owen, T. C.; Barltrop, J. A.; Cory, J. G. Use of an aqueous soluble tetrazolium/formazan assay for cell growth assays in culture. *Cancer Commun.* **1991**, *3*, 207–212.
- (36) Bonne, D.; Heusele, C.; Simon, C.; Pantaloni, D. 4',6-Diamidino-2-phenylindole, a fluorescent probe for tubulin and microtubules. *J. Biol. Chem.* **1985**, *260*, 2819–2825.

JM0704189